Evaluation of the head-helmet sliding properties in an impact test

Antonia Trotta[1], Aisling Ní Annaidh[1,2], Roy Owen Burek[3,4],Bart Pelgrims[5], Jan Ivens[5]

1 School of Mechanical & Materials Engineering, University College Dublin, Belfield, Dublin 4, Ireland

2 UCD Charles Institute of Dermatology, School of Medicine and Medical Science, University College Dublin, Belfield, Dublin 4, Ireland

3 Charles Owen & Co (Bow) Ltd, Croesfoel Industrial Park, Wrexham, LL14 4BJ

4 School of Engineering, Cardiff University, Queens Building, The Parade, Cardiff, CF24 3AA

5 KU Leuven, Department of Materials Engineering, Kasteelpark Arenberg 44, B-3001 Leuven, Belgium

Address for correspondence

Antonia Trotta

UCD School of Mechanical & Materials Engineering
University College Dublin
Belfield, Dublin 4, Ireland

Phone: +353 1 716 1978 - Fax number: +353 1 283 0534

Email: antonia.trotta@ucd.ie

Word count (Introduction through conclusion): 3992

Abstract

The scalp plays a crucial role in head impact biomechanics, being the first tissue involved in the impact and providing a sliding interface between the impactor and/or helmet and the skull. It is important to understand both the scalp-skull and the scalp-helmet sliding in order to determine the head response due to an impact. However, experimental data on the sliding properties of the scalp is lacking. The aim of this work was to identify the sliding properties of the scalp using cadaver heads, in terms of scalp-skull and scalp-liner (internal liner of the helmet) friction and to compare these values with that of widely used artificial headforms (HIII and magnesium EN960). The effect of the hair, the direction of sliding, the speed of the test and the normal load were considered. The experiments revealed that the sliding behaviour of the scalp under impact loading is characterised by three main phases: 1) the low friction sliding of the scalp over the skull (scalp-skull friction), 2) the tensioning effect of the scalp and 3) the sliding of the liner fabric over the scalp (scalp-liner friction). Results showed that the scalp-skull coefficient of friction (COF) is very low (0.06±0.048), whereas the scalp-liner COF is 0.29±0.07. The scalp-liner COF is statistically different **from** the value of the HIII-liner (0.75±0.06) and the magnesium **EN960**-liner (0.16±0.026). **These** data will lead to the improvement of current headforms for head impact standard tests, ultimately leading to more realistic head impact simulations and the optimization of helmet designs.

Keywords: Scalp, friction, head impact, helmet, rotational acceleration

1. Introduction

Traumatic Brain Injury (TBI) is the leading cause of death for young adults (under 45 years of age) worldwide (Gennarelli 1993, Jennett 1998, Coronado et al. 2015, Taylor 2017). Helmets are effective in reducing **head** accelerations and velocities, and can therefore contribute to the reduction of head and brain injuries in sport under some (but not all) conditions (Thompson and Patterson 1998, Povey et al. 1999, Thompson et al. 1999, Attewell et al. 2001, Keng 2005, Amoros et al. 2012, Hasler et al. 2015). The majority of helmet standard tests measure the reduction in linear acceleration to assess the quality of a helmet (Connor et al. 2016), despite a number of studies suggesting that the rotational acceleration is a better indicator of brain injury (Holbourn 1943, Gennarelli et al. 1987, Kleiven 2007, Forero Rueda et al. 2011, Kleiven 2013). The brain **is hypothesised to be** more sensitive to shear forces resulting from rotational and linear acceleration, than to compressive forces due to linear acceleration alone **(Adams et al. 1982, Gennarelli et al. 1982)**. Under these assumptions, researchers are now developing new helmet standard tests which incorporate the effect of rotational accelerations. The National Operating Committee for Standards in Athletic Equipment released a new standard for headgear which consists of a linear impactor test evaluating the rotational accelerations which will become active in 2018 (NOCSAE 2018). This will ultimately lead to helmet designs which are optimised to protect the head against both linear and rotational accelerations. Head-helmet sliding properties represent one of the parameters to consider when optimizing a helmet against rotational acceleration. Using two popular headforms, EN960 Magnesium headform and Hybrid III dummy headform (HIII), a number of authors have examined the effect of the headform-helmet friction over the years (Aare and Halldin 2003, Finan et al. 2008, Halldin and Kleiven 2013). The EN960 Magnesium headform does not have an outer layer to simulate scalp tissue; whereas the Hybrid III dummy

50 headform has a vinyl skin**.** Some researchers have claimed that a lower head-helmet friction
51 reduces the rotational acceleration undergone by the head during the impact and therefore
52 the risk of head injury (Aare and Halldin 2003, Halldin and Kleiven 2013, Halldin et al. 2013).
53 On the other hand, other works have claimed that a lower head-helmet friction, in some
54 cases, increases the rotational acceleration undergone by the head, depending on impact
55 location and angle (Finan et al. 2008, Ebrahimi et al. 2015). Despite the different opinions on
56 the effect of a lower head-helmet COF, researchers concluded that the material covering the
57 headform, and its sliding properties, are important in determining the head response in
58 oblique helmet impacts (Ebrahimi et al. 2015).

59 From this perspective, the knowledge of the sliding properties of the scalp is essential for a
60 better understanding of the impact biomechanics. The scalp is the most external part of the
61 head and is the first tissue involved in a head impact. It is free to slide over the skull and it is
62 anteriorly connected with the orbicularis oculi muscles, laterally connected to the frontal
63 process of the zygoma, to the superior aspect of the zygomatic arch and over the mastoid
64 process superior to the attachments of the sternocleidomastoid and trapezius muscles, and
65 in the back of the head it fuses with the superior nuchal line (Tolhurst et al. 1991). Therefore,
66 there are two primary surface interactions at play during an impact, the scalp-skull friction
67 and the scalp-helmet friction.

68 In the majority of cases, sliding properties of the skin are determined using the ASTM D3702
69 (Comaish and Bottoms 1971, Kondo 2002) or the ASTM D1894 (Gerhardt et al. 2008) standard
70 test. The ASTM D3702 involves the application of a rotational probe to test a surface using
71 the torque to determine the horizontal friction force. The ASTM D1894, instead, involves the
72 application of a translational motion of the probe on a surface to determine the static and

dynamic friction. Different normal loads and speeds can be applied in both cases. In the case of a head impact the helmet slides over the scalp and this sliding motion can be better represented using the ASTM D1894. This standard test allows the application of larger sliding distances and minimize unpredictable effects due to the presence of hair.

A number of studies have focused on the COF of the skin, concluding that skin friction depends on the type and physical properties of the contacting materials, on the body region, on the physiological skin conditions (e.g. hydration state, sebum level) and on mechanical contact parameters (e.g. normal load, sliding velocity) (Zhang and Mak 1999, Tang et al. 2008, Derler and Gerhardt 2012); while ethnicity and gender do not affect the COF (Sivamani et al. 2003). Age does not affect the COF (Sivamani et al. 2003); however, late age (80 years in men, post menopause for women) has been shown to affect the sebum level (Pochi et al. 1979), which affects the COF. Researchers have generally performed friction tests under small contact pressure; Fotoh et al. (Fotoh et al. 2008) reports a COF of 0.8±0.5 between a steel sphere and the forehead under a normal force of 0.1 N, while Christensen et al. (Christensen and Nacht 1983) reports a COF of 0.12-0.22 between a Teflon wheel and the forehead under a normal force of 1.96 N. However, the contact pressure between the helmet and the scalp can reach values up to 0.7 MPa, which represents the plateau value for the expanded polystyrene (EPS) foam of the helmet (Di Landro et al. 2002). At this point, the foam deforms, absorbing a large amount of energy, without increasing the contact pressure on the head.

Currently sliding properties of the scalp are not accurately represented in either artificial headforms or numerical head models. Artificial headforms do not always include a scalp-like material (Magnesium EN960) and if they do, it is a polymeric layer rigidly attached to the headform (HIII, NOCSAE, FOCUS headforms). In numerical head models, scalp tissue is

generally modelled as a linear elastic material rigidly connected to the skull (Zhang et al. 2001, Horgan and Gilchrist 2003, Belingardi et al. 2005, Deck and Willinger 2008), except for the model developed by Kleiven et al. which represents the scalp with two layers, a hyperelastic and an elastic layer (Kleiven 2007, Fahlstedt et al. 2015).

The aim of this work is to determine the sliding properties at play between the internal liner of a helmet and cadaver human heads and compare them with the sliding properties of the magnesium EN960 and HIII headforms. The results presented here will lead to the development, or modification, of headforms for head impact standard tests **with the aim of improving** helmet design. **Additionally, they will be used in finite element simulations to better understand the effect of friction during a head impact.**

2. Methods

Friction tests were performed on cadaver human heads, Hybrid III headform (HIII) and magnesium EN960 headform at KU (Katholieke Universiteit) Leuven, Belgium.

2.1 *Head preparation*

The ethics committee within KU Leuven approved the use of human cadaver heads for testing (Ethical approval n. NH0192017-02-02). Five Caucasian human heads with hair were obtained from the KU Leuven Anatomy Centre (age 73-86); three males and two females. The heads were decapitated between the C4 and C5 vertebra and rinsed with a 0.9% NaCl solution via the vena jugularis and the carotis interna and externa. The blood vessels were emptied using a 55cc syringe with air. The blood vessels, the carotis and the jugularis were sealed with ethibond 2/0 to avoid extensive loss of body fluids. No fixation was used. The heads were subsequently packaged in an airtight bag and frozen at -18°C. Five days prior to testing, the

heads were brought to 2°C to allow slow defrosting and to preserve the quality. On the day of the experiment, the eyes and mouth were sealed with ethibond 2.0; the nose was not sealed to allow internal pressure release if needed. The heads were transported and stored in the test lab at 4°C until one hour before the start of the experiments. After performing the experimental tests on the head with hair, each head was shaved and the same experiments were performed on the shaved head at a room temperature of 21±2°C.

2.2 *Set-up description*

The customised experimental set-up was developed based on the ASTM D1894 friction test method. The set-up (Figure 1) consists of a Schenck horizontal fatigue machine (25 kN load cell) coupled with a pneumatic cylinder. The horizontal tensile machine has a maximum stroke of ± 12.5 mm and a maximum frequency of 10 Hz (depending on the stroke). The pneumatic cylinder was used to apply the normal load. Vertical load and horizontal displacement were applied simultaneously using a linear slide consisting of a miniature slide and a guide rail. The two rows of precision ball bearings give four point contact with the rail thus offering accuracy, stability and rigidity even when under complex or variable loads. The probe in contact with the head is a cylindrical steel probe (diameter of 20 mm) covered with a layer of helmet internal liner (Duplex 22, a 100% polyester fabric of 230 g/m², produced by Tiba Tricot SRL in Italy and supplied by AGV, Italy) and connected to the pneumatic cylinder through a 5 kN load cell. 20 mm diameter was selected so to minimize the curvature effect of the head and to ensure a constant pressure. Heads were secured using an EPS-bead filled vacuum bag to avoid movement of the head during testing.

2.3 *Test specifications*

The effect of different parameters on the COF was examined: the normal load, the presence of hair, the frequency of the test, the direction of sliding and the stroke of the test. The normal load applied was between 20-200 N, which corresponds to stress values between 0.06-0.64 MPa (values experienced by the head during an impact) (Di Landro et al. 2002). Tests were performed on heads with and without hair in two main directions, longitudinal (sagittal plane) and transverse (coronal plane) direction. **These directions were chosen to represent common head impact directions in sports.** Two main sets of experiments were conducted on the human heads: one set at 12 mm stroke and one set at 23 mm stroke. The 12 mm stroke allowed for the identification of the dynamic scalp-skull friction; the 23 mm stroke allowed for the identification of the static and dynamic scalp-liner friction.

12 mm stroke: Four different frequencies were tested, 0.5, 1, 3 **(only longitudinal direction)**, 5 Hz **(on the heads with hair only the longitudinal direction was tested)**. In this scenario, an additional set of experiments was conducted using double-sided tape instead of the internal liner of the helmet. This had the effect of rigidly adhering the impactor to the skin, and allowed us to clearly differentiate between two sliding interactions: the skull-scalp interaction and the scalp-liner interaction.

23 mm stroke: Due to limitations of the machine which resulted in significant inertial forces and noise at higher frequencies, only 0.5 Hz was tested. In this set of experiments, the sliding distance of the probe over the head was maximised.

When testing headforms (HIII and EN960) only a 12mm stroke was tested since there is no skull-scalp sliding present and the only interaction at play was the headform-liner friction.

In the present study, 297 tests were performed in total on the human cadaver heads and at least 25 tests on each of the artificial headforms. To take into account the internal friction of

the Schenck horizontal fatigue system, a number of cycles without load were conducted before applying the normal force. The system outputs the value of the normal force, the displacement and the horizontal force. The friction was calculated as the ratio between the horizontal force (corrected by the internal friction of the machine) and the normal force. A multi-way ANOVA test followed by a post hoc analysis was used to analyse the data in Matlab.

3. Results

3.1 Qualitative analysis

When the probe slides over the human head, three main phases can be identified: 1) the sliding of the scalp over the skull, 2) the tensioning effect of the scalp and 3) the sliding of the probe over the scalp. Figure 2 shows the horizontal to vertical force ratio graph over displacement for a 12 mm (b) and 23 mm (a) stroke test on the human head. The arrows on the graph indicate the impact points and the direction of the movement. At 12 mm stroke (b), the probe impacts the scalp almost in the centre position (denoted by ① in the Figure 2b). Horizontal motion requires very little force, due to the sliding of the scalp over the skull. As the displacement increases, the scalp is pulled along with the probe and is stretched, increasing the horizontal force and thus the apparent friction (②). However, there is no sliding between the probe and the scalp. Considering then the experiments at 23 mm stroke (a), the response is quite different. Here, the probe impacts the scalp (①) at the outermost position of the stroke and starts stretching the scalp (②). The reaction force of the scalp increases until this force is equal to $\mu_s * F_N$ (with μ_s static scalp-liner COF) (③). After this point, the probe starts sliding over the scalp (④) since the horizontal force is greater than $\mu_d * F_N$ (where μ_d is the dynamic scalp-liner COF). In the following cycles, the only effects at play are

185 the scalp-skull sliding (⑤) and the tensioning of the scalp (② dashed) as the horizontal to
186 vertical force ratio remains below the static scalp-liner COF.
187
188 Figure 3 represents the distance travelled by the probe before sliding begins. This distance is
189 larger when the movement is in the transverse direction than in the longitudinal direction.
190 Given that the probe must travel an average of 12mm before sliding of the probe relative to
191 the scalp begins, it is clear that the experiments at 12mm stroke do not include the effect of
192 the scalp-liner friction.

193 The same experiment conducted on the HIII and the magnesium EN960 results in a completely
194 different response (Figure 4). Firstly, as expected, the movement of the scalp over the skull is
195 absent; secondly, it is not possible to discern between a static and dynamic COF, because the
196 probe is already moving when it impacts on the headform. In the magnesium EN960
197 headform, the horizontal to vertical force ratio is almost constant, indicating there is a
198 constant sliding of the probe over the surface of the headform. In the HIII, a variation of the
199 horizontal to vertical force ratio is observed when the probe changes direction. This is
200 probably due to indentation and shearing effects of the vinyl skin (PVC Plastisol 55A Shore)
201 covering the headform. When the force ratio reaches the friction coefficient, the probe starts
202 to slide over the vinyl skin, with a constant friction value.

203 3.2 Quantitative *Analysis*

204 Data was analysed depending on the shape of the friction response. The headform-liner COF
205 has been calculated as the average value of the flat region of the graph in Figure 4. For the
206 human head tests, the static and dynamic scalp-liner friction coefficients were determined
207 from the 23 mm stroke tests. Whereas the scalp-skull COF was calculated from both 12 and

23 mm stroke tests. The static scalp-liner COF corresponds to the maximum value of the friction in the first cycle after impact of the 23 mm stroke test. The dynamic scalp-liner friction has been calculated as the average value of the flat part of the friction curve in the first half cycle after impact. The scalp-skull COF has been determined as the average value of the friction in the interval of the impact point ± 1 mm for the 12 mm stroke tests, and as the average value of the flat region of the friction curve after the first cycle for the 23 mm stroke.

Scalp-skull friction

Figure 5 shows the average and standard deviation of the scalp-skull COF at different frequencies. The overall trend indicates that both the average value of the scalp-skull friction and the standard deviation increase with the frequency. Figure 6 shows values of COF versus the normal load at 0.5 Hz (a), 1 Hz (b), 3 Hz (c), and 5 Hz (d). Average and standard deviation of the COF in the different test configurations are shown in Table 1. At 0.5 and 1 Hz the value of the friction coefficient is almost constant at different normal loads. At 3 and 5 Hz, the friction decreases with the increase in normal load and it is lower than 0.1 around pressures of 0.7 MPa. This suggests that at increased frequencies, the scalp-skull friction is more sensitive to the normal load. Statistical analyses showed that the presence of the hair and the direction of sliding during testing do not affect the skull-scalp friction. Moreover, tests performed using double-sided tape (where only the skull-scalp friction is at play) gave the same results as the tests with the internal liner, leading to the conclusion that for 12 mm stroke there was no scalp-probe sliding.

Scalp-liner friction

Figure 7 shows the values of static and dynamic scalp (or headform)-liner COFs for the different headforms and for the human heads in four different configurations: with hair and

longitudinal direction (Hair/L), with hair and transverse direction (Hair/T), shaved head and longitudinal direction (Shaved/L), and shaved head and transverse direction (Shaved/T). Average values of the static scalp-liner COF are between 0.21 (Hair/T) and 0.35 (Shaved/T). Average values of the dynamic scalp-liner COF are between 0.20 (Hair/T) and 0.32 (Shaved/T). Average and standard deviation of the different configurations are shown in Table 2. The direction of sliding does not statistically affect the COF (static COF *p-value* 0.49, dynamic COF *p-value* 0.54), however, the presence of hair significantly reduces the COF (static COF *p-value* 1.46e-5, dynamic COF *p-value* 0.0008). The scalp-liner COF of human heads was statistically different (*p-value* 7.61e-31) when compared with the COF between the liner and the headforms (HIII and magnesium EN960). Values of the headform-liner friction are: 0.75±0.06 for the HIII and 0.16±0.026 for the magnesium EN960.

4. **Discussion**

In the first set of tests (12 mm stroke) on the human heads there was no sliding between the probe and the scalp. This was confirmed when the tests were repeated with the probe rigidly adhered to the scalp. The only sliding at play was that of the scalp over the skull. The average value of the scalp-skull friction was 0.06±0.048. The scalp-skull friction is not sensitive to the normal load at low frequencies but at higher frequencies (5 Hz) the COF decreases as the normal load increases. Tests performed in different configurations of the head showed that the scalp-skull friction does not depend on the presence of hair or on the direction of sliding.

A larger stroke (23 mm) allowed for the identification of the static and dynamic scalp-liner COF. In this case, as the probe pulls the scalp in tension, eventually the tangential force exceeds the normal force times the static scalp-liner friction ($F_H > \mu_s F_N$) allowing the probe to

slide over the scalp. Once the sliding starts the maximum tension applied to the skin is lower than the normal force times the static scalp-liner friction ($F_H<\mu_S F_N$). Therefore, in the cycles following the first one, the only effects at play are the scalp-skull sliding and the tensioning of the scalp. The different test configurations showed that the presence of hair reduces the scalp-liner COF but the direction of sliding does not have a significant effect. The difference in distances before sliding initiates is related to the mechanical properties of the scalp. Indeed, the scalp is anisotropic and the collagen fibres are oriented in the sagittal plane of the head (Langer 1861). Since the tissue is stiffer in the direction of the collagen fibres (Ní Annaidh et al. 2012), less displacement is necessary to reach higher forces. In the transverse direction, however, the scalp is softer and to obtain sliding, a larger displacement is necessary.

Tests performed on the artificial headforms (HIII and EN960) showed a different friction response and different headform-liner COF. In particular, the shape of the friction response does not include the tensioning effect of the skin since there is no skin-like material in the magnesium EN960. While it is sometimes claimed that the rubber material of the HIII is like skin, it is very thick and the friction coefficient between the aluminium and the rubber is significantly higher than the scalp-skull friction coefficient observed in this research. Therefore, the artificial skin on the HIII does not accurately represent human scalp-skull behaviour. The values of the headform-liner COFs vary considerably between the different headforms (0.75±0.06 for the HII and 0.16±0.03 for the magnesium EN960) and are statistically different when compared with the value of the human head (0.29±0.07). The low COF would induce too much sliding of the headform in the helmet during rotational impact, thus artificially reducing rotational accelerations. On the other hand, the COF of the rubber skin of the HIII is unrealistically high, reducing head-helmet displacement during rotational impact compared to a human head. This has significant consequences for those charged with

improving helmet standard tests, as artificial headforms should seek to replicate the sliding properties of a human head as closely as possible in order to replicate realistic head impacts.

Replicating the sliding properties will affect the kinematics of the head and therefore the rotational acceleration undergone by the head during an impact. FE head models should change the scalp boundary conditions and artificial headforms should adopt a soft layer with a COF closer to the human scalp. New helmets should be optimised taking into account the sliding of the scalp, which could result in new helmet designs. Liner materials should be chosen considering both comfort and scalp-liner friction, with the aim to reduce the effect of the rotational acceleration.

Limitations of the work include the age of the heads (only elderly subjects in this study), the type of hair (Caucasian straight hair), the physiological skin condition, the fact that the effect of the sweat and the sebum level of the scalp were not considered and only one location on the head (vertex location) was tested because it is reasonably flat. Additionally, only frequencies up to 5 Hz for the 12 mm stroke and 0.5 Hz for 23 mm stroke were tested due to limitations caused by the inertia of the test set-up. It is known that the mechanical properties of the scalp depend on the strain rate (Ottenio et al. 2015); the scalp becomes stiffer at high strain rates. This would result in an increased stress build-up in the scalp and a shorter distance before the probe starts sliding. Moreover at high frequencies the COF becomes highly dependent on the normal load. However the values of COF at 5 Hz and 0.6-0.7 MPa of normal load seem to be comparable with the value of the COF at lower frequencies. Future research should investigate the COF of other materials used as comfort padding (for instance VN or EPP used in hockey and American football helmets) and higher frequencies.

5. Conclusion

During the test, three main phases were identified: sliding of the scalp over the skull with a low COF (0.06±0.048); tensioning of the scalp; and sliding of the internal liner over the scalp (COF of 0.29±0.07). Neither the presence of hair, the frequency of the test, nor the direction of sliding had an effect on the scalp-skull COF. However, the presence of hair does reduce the static and dynamic scalp-liner COF. The normal load was found to affect the COF, but only at high frequencies. Comparing the head with the artificial headforms, there are two main differences: 1) the headforms do not include a scalp-skull friction and therefore there is no tensioning effect of the skin; 2) the scalp-liner COF (0.29±0.07) is statistical different (*p-value* 7.61e-31) from the headform-liner COF, in particular the HIII has a very high friction coefficient (0.75±0.06) that is more than twice the scalp-liner COF and the magnesium EN960 has a COF lower than the human head (0.16±0.03).

Acknowledgements

Funding was provided by the European Union's Horizon 2020 research programme under the Marie Sklodowska – Curie grant agreement No. 642662. The authors wish to thank Bart Depreitere, the ethical committee of KU Leuven and the anatomy skills centre for their support and approval.

Conflict of interest

The authors have no relevant conflict of interest to report.

References

Aare, M. and Halldin, P., 2003. A new laboratory rig for evaluating helmets subject to oblique impacts. Traffic injury prevention 4(3): 240-248.

Adams, J. H., Graham, D., Murray, L. S. and Scott, G., 1982. Diffuse axonal injury due to nonmissile head injury in humans: an analysis of 45 cases. Annals of neurology 12(6): 557-563.

Amoros, E., Chiron, M., Martin, J.-L., Thélot, B. and Laumon, B., 2012. Bicycle helmet wearing and the risk of head, face, and neck injury: a French case–control study based on a road trauma registry. Injury Prevention 18(1): 27-32.

Attewell, R. G., Glase, K. and McFadden, M., 2001. Bicycle helmet efficacy: a meta-analysis. Accident Analysis & Prevention 33(3): 345-352.

Belingardi, G., Chiandussi, G. and Gaviglio, I., 2005. Development and validation of a new finite element model of human head. Proc. 19th International Technical Conference of the Enhanced Safety of Vehicle (ESV), Washington, DC,

Christensen, M. S. and Nacht, S., 1983. Facial oiliness and dryness: correlation between instrumental measurements and self-assessment.

Comaish, S. and Bottoms, E., 1971. The skin and friction: deviations from Amonton's laws, and the effects of hydration and lubrication. British Journal of Dermatology 84(1): 37-43.

Connor, T. A., Meng, S. and Zouzias, D., 2016. Current Standards for Sports and Automotive Helmets: A Review.

Coronado, V. G., Haileyesus, T., Cheng, T. A., Bell, J. M., Haarbauer-Krupa, J., Lionbarger, M. R., Flores-Herrera, J., McGuire, L. C. and Gilchrist, J., 2015. Trends in sports-and recreation-related traumatic brain injuries treated in US emergency departments: the National Electronic Injury Surveillance System-All Injury Program (NEISS-AIP) 2001-2012. The Journal of head trauma rehabilitation 30(3): 185-197.

Deck, C. and Willinger, R. m., 2008. Improved head injury criteria based on head FE model. International Journal of Crashworthiness 13(6): 667-678.

Derler, S. and Gerhardt, L.-C., 2012. Tribology of skin: review and analysis of experimental results for the friction coefficient of human skin. Tribology Letters 45(1): 1-27.

Di Landro, L., Sala, G. and Olivieri, D., 2002. Deformation mechanisms and energy absorption of polystyrene foams for protective helmets. Polymer testing 21(2): 217-228.

Ebrahimi, I., Golnaraghi, F. and Wang, G. G., 2015. Factors influencing the oblique impact test of motorcycle helmets. Traffic injury prevention 16(4): 404-408.

Fahlstedt, M., Depreitere, B., Halldin, P., Vander Sloten, J. and Kleiven, S., 2015. Correlation between injury pattern and finite element analysis in biomechanical reconstructions of traumatic brain injuries. Journal of biomechanics 48(7): 1331-1335.

Finan, J. D., Nightingale, R. W. and Myers, B. S., 2008. The influence of reduced friction on head injury metrics in helmeted head impacts. Traffic injury prevention 9(5): 483-488.

Forero Rueda, M. A., Cui, L. and Gilchrist, M. D., 2011. Finite element modelling of equestrian helmet impacts exposes the need to address rotational kinematics in future helmet designs. Computer methods in biomechanics and biomedical engineering 14(12): 1021-1031.

Fotoh, C., Elkhyat, A., Mac, S., Sainthillier, J. M. and Humbert, P., 2008. Cutaneous differences between black, African or Caribbean mixed-race and Caucasian women: biometrological approach of the hydrolipidic film. Skin Research and Technology 14(3): 327-335.

Gennarelli, T. A., 1993. Mechanisms of brain injury. The Journal of emergency medicine 11: 5-11.

Gennarelli, T. A., Thibault, L. E., Adams, J. H., Graham, D. I., Thompson, C. J. and Marcincin, R. P., 1982. Diffuse axonal injury and traumatic coma in the primate. Annals of neurology 12(6): 564-574.

Gennarelli, T. A., Thibault, L. E., Tomei, G., Wiser, R., Graham, D. and Adams, J., 1987. Directional dependence of axonal brain injury due to centroidal and non-centroidal acceleration.

Gerhardt, L. C., Mattle, N., Schrade, G., Spencer, N. and Derler, S., 2008. Study of skin–fabric interactions of relevance to decubitus: friction and contact-pressure measurements. Skin Research and Technology 14(1): 77-88.

Halldin, P. and Kleiven, S., 2013. The development of next generation test standards for helmets. Proceedings of the 1st International Conference on Helmet Performance and Design,

Halldin, P., Lanner, D., Coomber, R. and Kleiven, S., 2013. Evaluation of blunt impact protection in a military helmet designed to offer blunt and ballistic impact protection. Childs PRN, Bull A, Ghajari M, editors. Proceedings of the first International Conference on Helmet Performance and Design,

Hasler, R. M., Baschera, D., Taugwalder, D., Exadaktylos, A. K. and Raabe, A., 2015. Cohort study on the association between helmet use and traumatic brain injury in snowboarders from a Swiss tertiary trauma center. World neurosurgery 84(3): 805-812.

Holbourn, A., 1943. Mechanics of head injuries. The Lancet 242(6267): 438-441.

Horgan, T. and Gilchrist, M. D., 2003. The creation of three-dimensional finite element models for simulating head impact biomechanics. International Journal of Crashworthiness 8(4): 353-366.

Jennett, B., 1998. Epidemiology of head injury. Archives of Disease in Childhood 78(5): 403-406.

Keng, S.-H., 2005. Helmet use and motorcycle fatalities in Taiwan. Accident Analysis & Prevention 37(2): 349-355.

Kleiven, S., 2007. Predictors for traumatic brain injuries evaluated through accident reconstructions. Stapp car crash journal 51: 81.

Kleiven, S., 2013. Why most traumatic brain injuries are not caused by linear acceleration but skull fractures are. Frontiers in bioengineering and biotechnology 1

Kondo, S., 2002. The Frictional Properties Between Fabrics and the Human Skin (Part 2): Influences of Stratum Corneum Water Content, Hardness of Skin, Friction Pressure, and Friction Speed on the Frictional Properties. JOURNAL-JAPAN RESEARCH ASSOCIATION FOR TEXTILE END USES 43(5): 41-57.

Langer, K., 1861. On the anatomy and physiology of the skin. The Imperial Academy of Science, Vienna. British Journal of Plastic Surgery 17(31): 93-106.

Ní Annaidh, A., Bruyere, K., Destrade, M., Gilchrist, M. D., Maurini, C., Otténio, M. and Saccomandi, G., 2012. Automated estimation of collagen fibre dispersion in the dermis and its contribution to the anisotropic behaviour of skin. Annals of biomedical engineering 40(8): 1666-1678.

NOCSAE, 2018. Standard pneumatic ram test method and equipment used in evaluating the performance characteristics of protective headgear and face guards.

Ottenio, M., Tran, D., Annaidh, A. N., Gilchrist, M. D. and Bruyère, K., 2015. Strain rate and anisotropy effects on the tensile failure characteristics of human skin. Journal of the mechanical behavior of biomedical materials 41: 241-250.

Pochi, P. E., Strauss, J. S. and Downing, D. T., 1979. Age-related changes in sebaceous gland activity. Journal of Investigative Dermatology 73(1): 108-111.

Povey, L. J., Frith, W. and Graham, P., 1999. Cycle helmet effectiveness in New Zealand. Accident Analysis & Prevention 31(6): 763-770.

Sivamani, R. K., Wu, G. C., Gitis, N. V. and Maibach, H. I., 2003. Tribological testing of skin products: gender, age, and ethnicity on the volar forearm. Skin Research and Technology 9(4): 299-305.

Tang, W., Ge, S.-r., Zhu, H., Cao, X.-c. and Li, N., 2008. The influence of normal load and sliding speed on frictional properties of skin. Journal of bionic engineering 5(1): 33-38.

Taylor, C. A., 2017. Traumatic brain injury–related emergency department visits, hospitalizations, and deaths—United States, 2007 and 2013. MMWR. Surveillance Summaries 66

Thompson, D. C. and Patterson, M. Q., 1998. Cycle helmets and the prevention of injuries. Recommendations for competitive sport.

Thompson, D. C., Rivara, F. P. and Thompson, R., 1999. Helmets for preventing head and facial injuries in bicyclists. Cochrane database of systematic reviews 4(2)

Tolhurst, D. E., Carstens, M. H., Greco, R. J. and Hurwitz, D. J., 1991. The surgical anatomy of the scalp. Plastic and reconstructive surgery 87(4): 603-612.

Zhang, L., Yang, K. H., Dwarampudi, R., Omori, K., Li, T., Chang, K., Hardy, W. N., Khalil, T. B. and King, A. I., 2001. Recent advances in brain injury research: a new human head model development and validation. Stapp Car Crash J 45(11): 369-394.

Zhang, M. and Mak, A., 1999. In vivo friction properties of human skin. Prosthetics and orthotics International 23(2): 135-141.

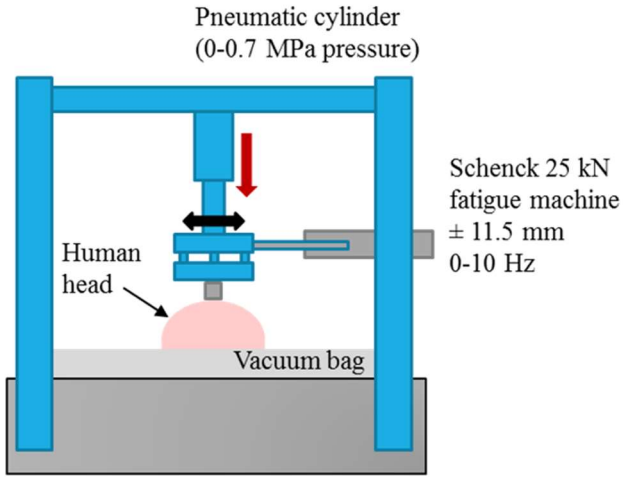

Figure 1: Experimental set-up for the friction tests.

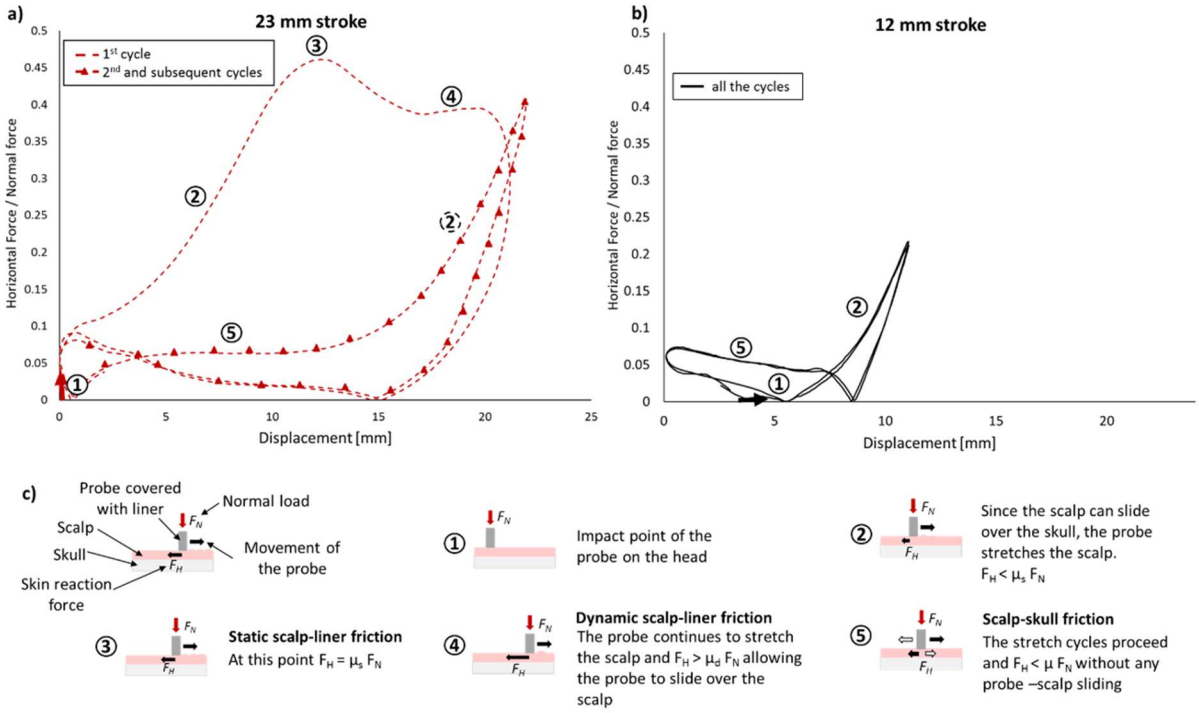

Figure 2: Representative friction coefficient-displacement graph of the human head for 23 mm (a) and 12 mm (b) stroke, followed by an explanation of the different phases of the test (c). ***The ratio between horizontal and normal force (y axis) is non-dimensional****. Each phase is associated with a number (1-5). μ_s is the static scalp-liner friction, μ_d is the dynamic scalp-liner friction, μ is the scalp-skull friction. The 1st cycle of the 23mm stroke (a) differs considerably from the 2nd and subsequent cycles. In the 1st cycle of the 23 mm stroke, the static (③) and dynamic (④) scalp-liner friction can be identified, in the 2nd and subsequent cycles, the scalp-skull friction (⑤) and the skin tension (② dashed) are the only effects at play and there is no sliding of the probe relative to the scalp. At 12 mm stroke (b), the reaction force of the skin is not sufficient to overcome $\mu_s F_N$ and the identification of the static and dynamic scalp-liner*

friction is not possible; in this case the tensioning of the skin (②) and the scalp-skull friction (⑤) are the only phases.

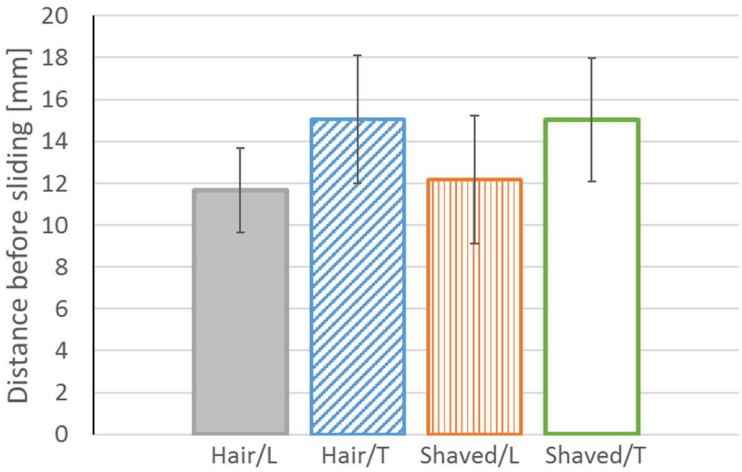

Figure 3: Distance before the probe starts sliding over the scalp in different configurations.

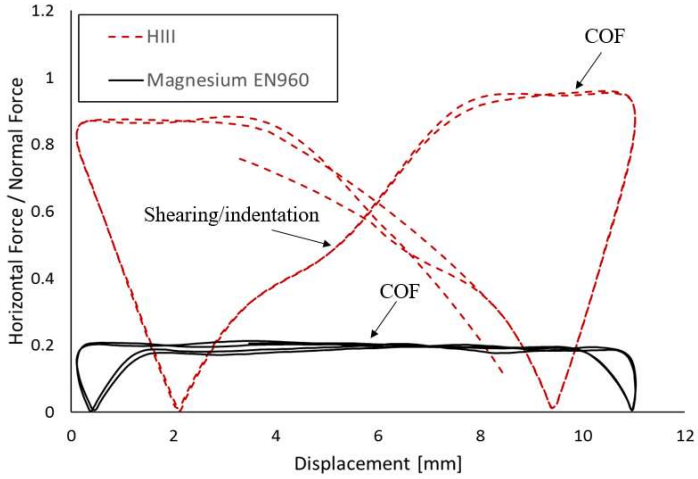

Figure 4: Representative friction coefficient-displacement graph for the HIII (dashed line) and magnesium EN960 (continuous line). ***The ratio between horizontal and normal force (y axis) is non-dimensional.*** *Only the headform-liner COF can be identified in the case of EN960. For the HIII, two main effects can be identified: the shearing/small indentation of the rubber material and the headform-liner COF.*

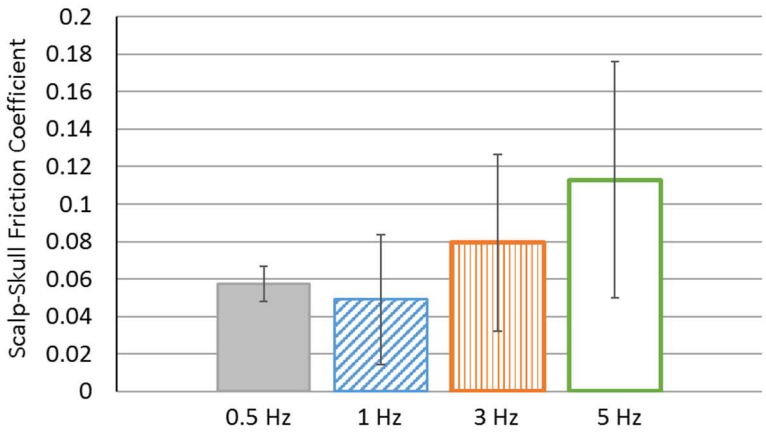

Figure 5: Scalp-skull friction coefficient at different frequencies (average ± standard deviation).

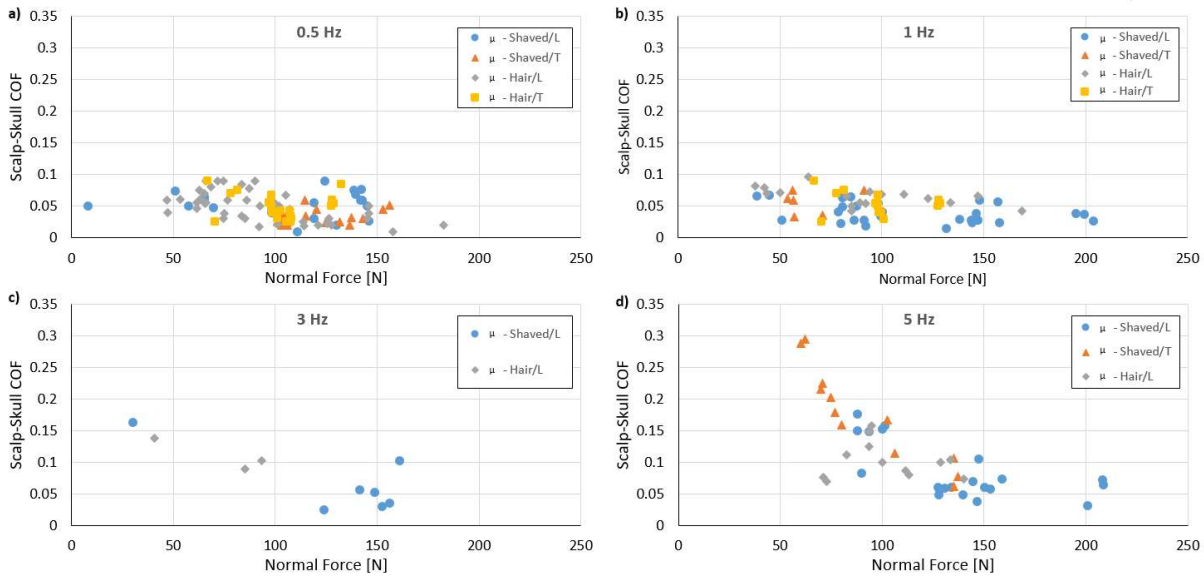

*Figure 6: Scalp-skull COF of the human head versus normal load graph at **0.5 Hz (a), 1 Hz (b), 3 Hz (c), and 5 Hz (d)**. **Four** different head configurations have been reported in these graphs: shaved/L (shaved head and longitudinal direction), Shaved/T (shaved head and transverse direction), Hair/L (head with hair and longitudinal direction) **and Hair/T (head with hair and transverse direction)**. **At 0.5 and 1 Hz (a-b) the friction does not depend on the load. At 3 and 5 Hz (b) the friction value decreases with the increase in normal force.***

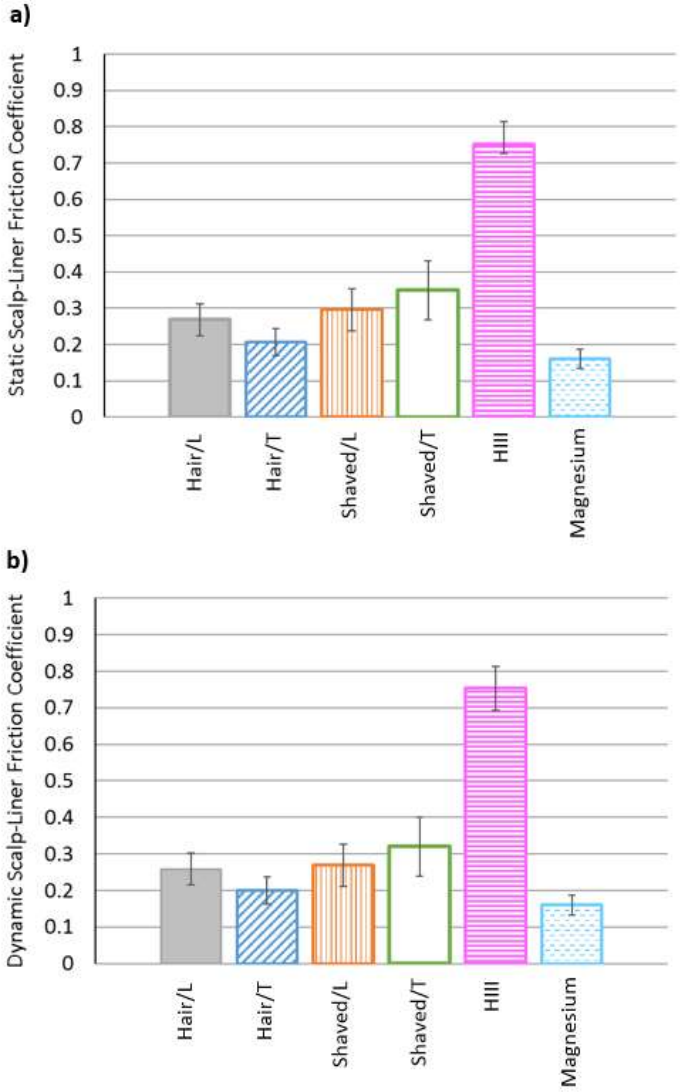

Figure 7: Static (a) and Dynamic (b) scalp/surface-liner friction coefficient of the human head (in different configurations) and of widely used artificial headforms (HIII and magnesium EN960).